

# Frequency-tunable bandstop-bandpass dual-function microwave filter

Kangho Lee<sup>1</sup>, Tae-Hak Lee<sup>1</sup>, Gyu Churl Park<sup>2</sup>,  
Hjalti H. Sigmarsson<sup>3</sup>, and Juseop Lee<sup>1a)</sup>

<sup>1</sup> Korea University, 145 Anam-ro, Seongbuk-gu, Seoul, 136–701, Republic of Korea

<sup>2</sup> Agency for Defense Development,

P.O. Box 35, Yuseong-gu, Daejeon, 305–600, Republic of Korea

<sup>3</sup> The University of Oklahoma, 3190 Monitor Avenue, Norman, OK 73019, USA

a) [juseoplee@korea.ac.kr](mailto:juseoplee@korea.ac.kr)

**Abstract:** This letter presents a frequency-tunable, dual-function, microwave filter with both bandpass and bandstop functionalities. The filter uses a single switch to change the functionality minimizing the insertion loss, and it can replace a traditional filter bank structure that contains two filters and two switches. Frequency-tunable substrate-integrated waveguide (SIW) resonators are adopted in this filter design. Measured results show that both bandpass and bandstop responses can be tuned from 3.0 GHz to 3.6 GHz. The measured minimum insertion loss at the center frequency is 1.1 dB for the bandpass mode and the attenuation at the center frequency is greater than 40 dB over the entire frequency tuning range.

**Keywords:** filter, microwave, bandpass, bandstop, tunable

**Classification:** Microwave and millimeter wave devices, circuits, and systems

## References

- [1] M. Sánchez-Renedo, R. Gómez-García, J. I. Alonso and C. Briso-Rodríguez: IEEE Trans. Microw. Theory Techn. **53** (2005) 191. DOI:10.1109/TMTT.2004.839309
- [2] B. Yassini, M. Yu and B. Keats: IEEE Trans. Microw. Theory Techn. **60** (2012) 4002. DOI:10.1109/TMTT.2012.2224367
- [3] H. Joshi, H. H. Sigmarsson, S. Moon, D. Peroulis and W. J. Chappell: IEEE Trans. Microw. Theory Techn. **57** (2009) 3525. DOI:10.1109/TMTT.2009.2034309
- [4] J. Lee, E. J. Naglich and W. J. Chappell: IEEE Microw. Wireless Compon. Lett. **20** (2010) 669. DOI:10.1109/LMWC.2010.2080669
- [5] E. J. Naglich, J. Lee, D. Peroulis and W. J. Chappell: IEEE Trans. Microw. Theory Techn. **58** (2010) 3770. DOI:10.1109/TMTT.2010.2086533
- [6] J. Lee, E. J. Naglich, H. H. Sigmarsson, D. Peroulis and W. J. Chappell: IEEE Trans. Microw. Theory Techn. **61** (2013) 1114. DOI:10.1109/TMTT.2012.2237036
- [7] J.-S. Hong and M. J. Lancaster: *Microstrip Filters for RF/Microwave Applications* (John Wiley & Sons, New York, 2001).

- [8] R. J. Camerson, C. M. Kudsia and R. R. Mansour: *Microwave Filters for Communications Systems* (Wiley Interscience, 2007).

## 1 Introduction

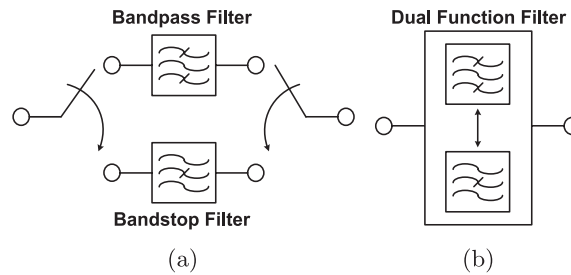
As next-generation communications systems are required to be adaptive to the frequency spectrum environment, development of frequency-tunable and reconfigurable filters has been of great interest. Hence, such filters using various types of resonators have been exploited and reported extensively. In [1], a combline filter structure with continuously tunable center frequency and bandwidth is presented. In [2], a Ka-band fully tunable waveguide cavity filter with a continuous tuning performance is reported. In addition, frequency-tunable substrate-integrated waveguide bandpass and bandstop filter structures with adjustable responses are described in [3, 4]. The aforementioned filters have capability of tuning their frequency responses, but they are not capable of changing functionality. Hence, studies have also been expanded to explore multifunction filter. In [5, 6], it is shown that reconfigurable filters can have two functionalities by utilizing a number of switches, but having multiple switches in filter structures is one of drawbacks sacrificing insertion loss performance.

This paper presents a frequency-tunable dual-function filter with a single switch and its design method. The presented filter can have either bandpass or bandstop response depending on the state of the switch. Substrate-integrated waveguide resonators are employed in this filter structure to achieve frequency tuning. The measured results of the designed filter verify that it can replace conventional filter banks in agile multi-functional systems that require advanced filter performance.

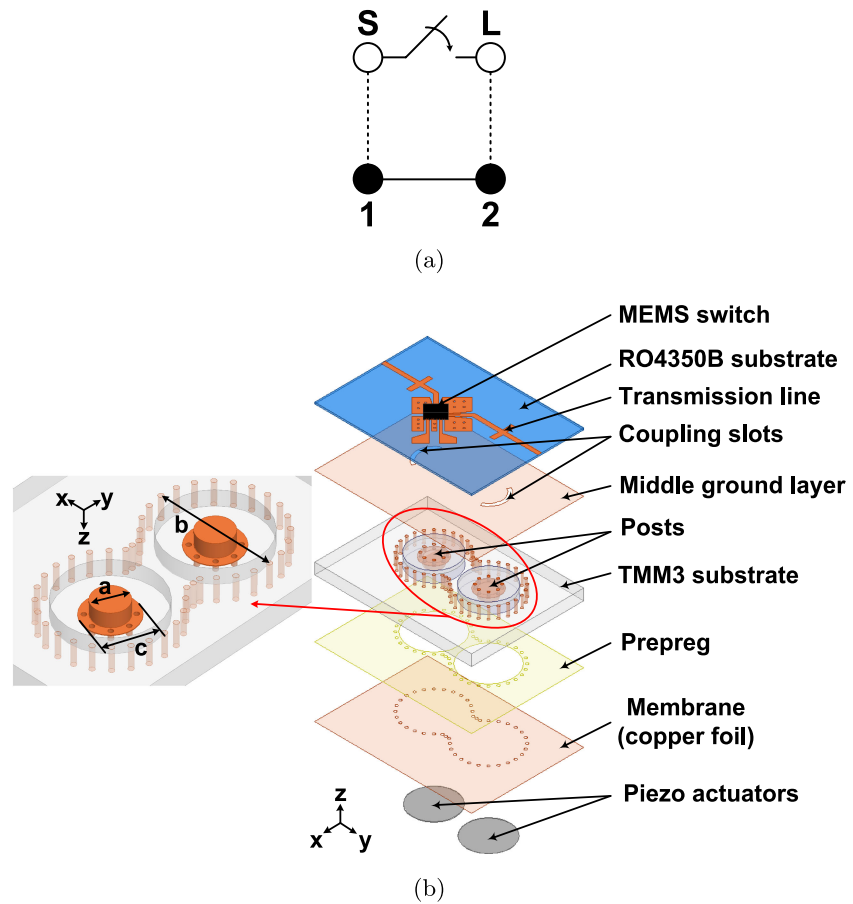
## 2 Filter structure and design

Fig. 1(a) shows the block diagram of a conventional filter bank having two filters. Bandpass and bandstop filters are connected in parallel having two switches, one at the input port and one at the output port. This filter bank can have either a bandpass or a bandstop response depending on the switch configuration. In this work, we design a single-switch, dual-function filter (Fig. 1(b)) capable of providing both bandpass and bandstop responses.

This work uses the filter topology shown in Fig. 2(a) and the filter structure in this work is shown in Fig. 2(b). The filter is composed of two substrates, Rogers RO4350B and TMM3. The microstrip line in the upper substrate runs from the input port to the output port, and a RF MEMS (microelectromechanical system) switch from OMRON (2SMES-01) is situated in the middle of the microstrip line. Two frequency-tunable post-loaded cylindrical cavity resonators are embedded in a 3.175 mm-thick TMM3 substrate. Air gaps are formed between the posts and the membrane due to the holes that are cut out in the prepreg layer. The capacitance between the post and the membrane can be controlled by moving the membrane, and this enables resonant frequency tuning. Taking this into account, the resonator dimensions have been determined based on the frequency tuning range



**Fig. 1.** (a) Block diagram of a conventional filter bank with two filters. (b) Block diagram of a dual function filter.



**Fig. 2.** (a) Filter topology for the dual function filter with a single switch. (b) Layer-by-layer view of the dual function filter using frequency tunable substrate-integrated waveguide resonators. ( $a = 4.6$  mm,  $b = 16$  mm,  $c = 7$  mm)

(3.0–3.6 GHz). The coupling slots on the ground plane are for the external coupling between the transmission line and each resonator. The inductive iris between the two resonators is the inter-resonator coupling structure.

The filter exhibits a bandpass response when the switch is off and the normalized  $(N + 2) \times (N + 2)$  coupling matrix has the form of

$$\mathbf{M}_p = \begin{bmatrix} 0 & M_{01p} & 0 & M_{03p} \\ M_{01p} & M_{11p} & M_{12p} & 0 \\ 0 & M_{12p} & M_{22p} & M_{23p} \\ M_{03p} & 0 & M_{23p} & 0 \end{bmatrix} \quad (1)$$

where  $M_{01p}$  is the normalized external coupling value between the input port and the resonator 1,  $M_{23p}$  is the one between the output port and the resonator 2, and  $M_{12p}$  is the normalized inter-resonator coupling value between the two resonators.  $M_{11p}$  and  $M_{22p}$  are the self-coupling values for the resonators 1 and 2, respectively, and they define the resonant frequency of each resonator.  $M_{03p}$  is the normalized coupling value between the input and output ports and is zero since the switch is in the off-state for the bandpass mode. In this work, we design the filter to have a second-order Butterworth response with 3.0% fractional bandwidth ( $\Delta f_p$ ) at 3.3 GHz. Filter synthesis for finding the normalized coupling values can be carried out by using the well-known filter synthesis methods [7, 8], and the values for the Butterworth response are given by  $M_{01p} = M_{23p} = 0.8409$ ,  $M_{12p} = 0.7071$ , and  $M_{11p} = M_{22p} = 0$ .

The filter exhibits a bandstop response when the switch is in the on-state and the coupling matrix has the form of

$$\mathbf{M}_s = \begin{bmatrix} 0 & M_{01s} & 0 & M_{03s} \\ M_{01s} & M_{11s} & M_{12s} & 0 \\ 0 & M_{12s} & M_{22s} & M_{23s} \\ M_{03s} & 0 & M_{23s} & 0 \end{bmatrix} \quad (2)$$

In this case,  $M_{03s}$  is unity since the switch is in the on-state for the bandstop mode. In this work, we design the filter to have a second-order Butterworth bandstop response with 3.3% fractional bandwidth ( $\Delta f_s$ ) at 3.3 GHz, and the values for the Butterworth response are given by  $M_{01s} = M_{23s} = 1.189$  and

$$M_{11s} = -M_{22s} = \pm \sqrt{M_{01s}^2 M_{12s} - M_{12s}^2} \quad (3)$$

where  $M_{12s}$  can be arbitrary as long as it is smaller than 1.414 [4]. Since  $M_{12s}$  for the bandstop mode can be chosen arbitrarily, the inter-resonator coupling structure can be designed based on the design parameters for the bandpass mode and reused for the bandstop mode.

The denormalized inter-resonator coupling value is then given by

$$k_{12p} = M_{12p} \Delta f_p = k_{12s} = M_{12s} \Delta f_s \quad (4)$$

and the inductive iris must be designed to satisfy the coupling value given in (4). The coupling value of the inductive iris can be conveniently controlled by the iris width and extracted from the resonant frequencies of the coupled resonator structure [7, 8]. Fig. 3 shows the top-view of the coupled resonator structure and the relationship between the iris width and the inter-resonator coupling value. Since the required inter-resonator coupling coefficient is 0.0212, the iris width has been determined to be 9.0 mm.

The denormalized external coupling values for the bandstop and bandpass modes are given by

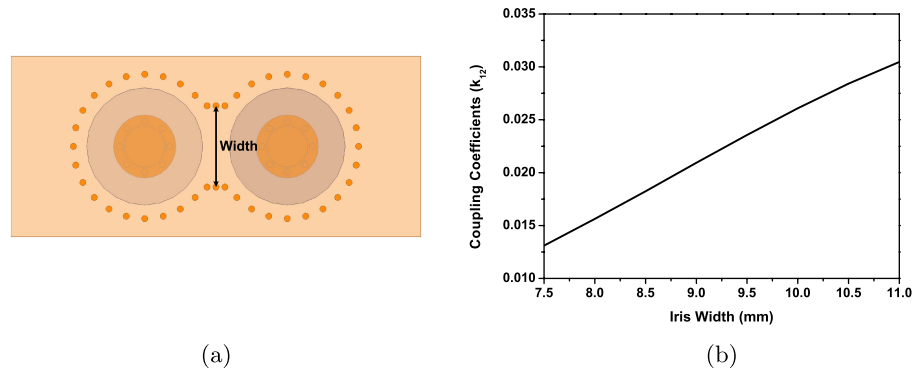


**Fig. 3.** (a) Structure for extracting the inter-resonator coupling value. (b) The relationship between the inter-resonator coupling value and the iris width.

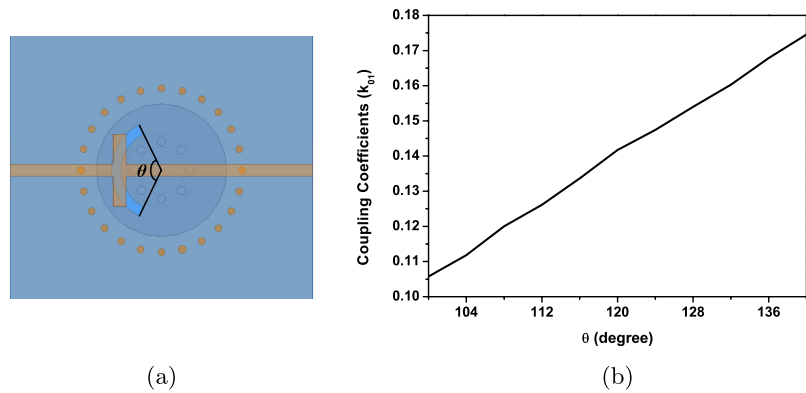


**Fig. 4.** (a) Structure for extracting the external coupling value for the bandstop mode. (b) The relationship between the external coupling value and the slot angle.

$$k_{01s} = M_{01s} \sqrt{\Delta f_s / 2} \quad (5)$$

$$k_{01p} = M_{01p} \sqrt{\Delta f_p},$$

respectively. The external coupling value for the bandstop mode is mainly determined by the size of the coupling slot, and that for the bandpass mode can be controlled by both the coupling slot size and the distance between the coupling slot and the open circuit (The switch is open for the bandpass mode). Hence, the size of the coupling slot must be determined to satisfy  $k_{01s}$  value and the length of an open-circuited stub extending beyond the coupling slot must be determined in a way that satisfies  $k_{01p}$  value. Fig. 4 shows the relationship between the external coupling value for the bandstop mode and the angle of the coupling slot. Since the required value for the external coupling for the bandstop mode is 0.1527, the slot angle has been chosen to be 128 degrees. Fig. 5 relates the external coupling value for the bandpass mode to the length of the open-circuited stub ( $l$  in Fig. 5) under the condition that the slot angle is 128 degrees. The required external value,  $k_{01p} = 0.1456$ , mandates that the length is 18.25 mm. Based on this analysis, we have designed the microstrip line structure containing the switch. The switch is not an ideal open circuit at off state and it has parasitic capacitance. This parasitic

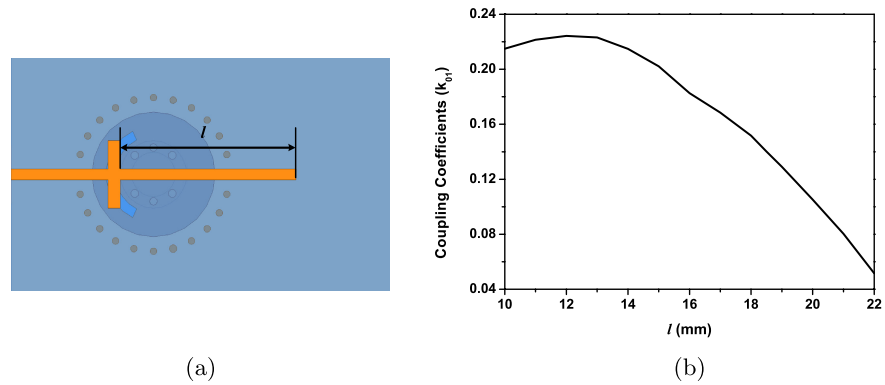


**Fig. 5.** (a) Structure for extracting the external coupling value for the bandpass mode. (b) The relationship between the external coupling value and the length of the open-ended microstrip line.

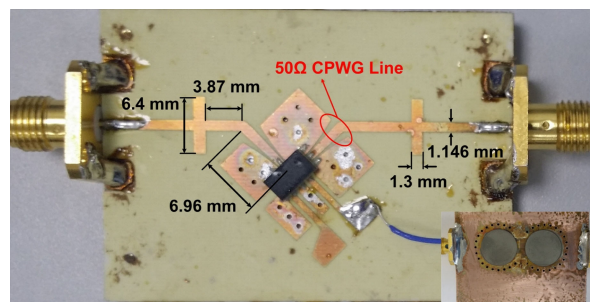


**Fig. 6.** Top- and bottom-views (inset) of the fabricated filter.

capacitance must be de-embedded, and the microstrip line length from the coupling slot to the switch is 10.83 mm after absorbing the parasitic capacitance which is smaller than 18.25 mm. The detailed dimensions for the microstrip line structure is given in Fig. 6.

### 3 Fabrication and measurement

The designed, single-switch, dual-function filter has been fabricated using milling, copper plating, etching, and laminating processes. Fig. 6 shows the top- and bottom-views of the fabricated filter. Fig. 7(a) shows the measured responses of the fabricated filter for the bandpass mode, and it also compares the measured response to the synthesized one at 3.3 GHz. The filter can be tuned from 3.0 to 3.6 GHz having the return loss better than 10 dB. The insertion loss at the center frequency is smaller than 1.7 dB over the entire frequency range. Fig. 7(b) shows the measured responses for the bandstop mode. The attenuation at the center frequency is measured to be greater than 40 dB over the entire frequency range and the insertion loss in the passband is less than 1.0 dB. The discrepancy between the measured and synthesized return losses for the bandstop mode can be attributed to the fact that the transmission line between the input and output ports has frequency-dependent characteristic while it is set to be frequency-independent in synthesis.

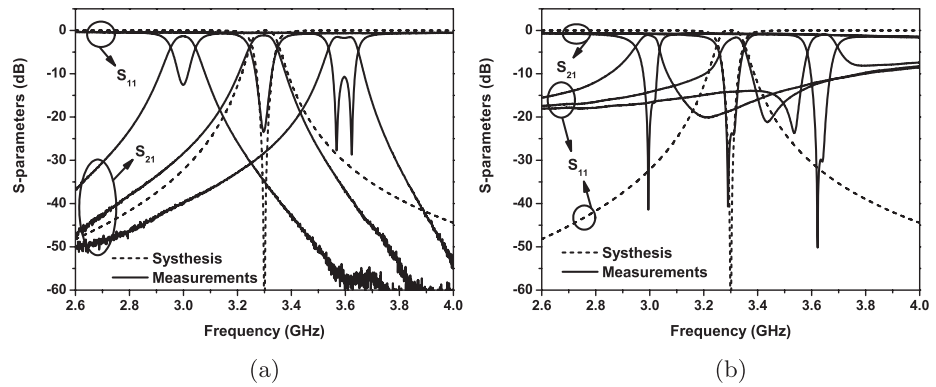


**Fig. 7.** Measured frequency response of the fabricated filter for the (a) bandpass mode and (b) bandstop mode.

#### 4 Conclusion

This paper presents a frequency-tunable dual function filter composed of a single MEMS switch and substrate-integrated waveguide resonators. A analytic design procedure are described for designing the dual function filter using a single switch. Both bandpass and bandstop responses can be obtained from the filter over the frequency tuning range from 3.0 GHz to 3.6 GHz, indicating that the presented filter can replace a filter bank having bandpass and bandstop filters connected in parallel. This work represents a significant step towards realizing advanced multi-functional filters that are going to be key components in spectrum-agile communications and radar systems of the future.

#### Acknowledgments

This work was supported by Agency for Defense Development (Contract Number: UD120046FD).